Indonesian Journal of Electrical Engineering and Informatics (IJEEI)
Vol.1, No.1, March 2013, pp. 1~7
ISSN: 2089-3272

A New Method for Recognition of Arcing Faults in Transmission Lines using Wavelet Transform and Correlation Coefficient

Navid Ghaffarzadeh
Technical and Engineering Faculty, Imam Khomeini International University, Qazvin, Iran
e-mail: ghaffarzadeh@ikiu.ac.ir

Abstract

In this paper a novel method based on discrete wavelet transform and correlation coefficient is presented for distinguishing between arcing and permanent faults. The algorithm includes offline and online processing. In the offline, discrete wavelet transform is used to decompose typical faulted phase voltage waveforms during arcing faults. An index is then defined and computed. The index is based on the normalised energy of detail coefficients at resolution levels 1 to 14. The online processing consists of capturing the faulted phase voltage waveform using a 20 kHz sampling rate, and decomposing it by db4. Finally, arcing faults are distinguished from permanent faults based on correlation coefficient of the computed index of the pre-stored typical arcing faults and a recorded indistinct signal. The effectiveness of the approach has been tested for numerous arcing and permanent fault conditions on a transmission line using the Electromagnetic Transient Program (EMTP) software tool. The simulation results show the capability of the proposed method in distinguishing between arcing faults from permanent faults.

Keywords: *arcing faults, transmission lines, discrete wavelet transform, correlation coefficient*

1. Introduction

According to the statistics data, about 70~80% of faults on transmission lines are single-phase to earth faults, which are mostly of transient (arcing) type. Distinguishing between transient and permanent faults for single pole auto-reclosing has therefore been the subject of several research works over the past 15 years. In [1] the neural network based technique was used to recognise transient faults. An arc-based scheme using the Fourier transform was proposed in [2]. Bo, et al used the transient high frequency signals of the faulted phase in [3-4], whereas in [5] they used the current of one of the two healthy phases and compared its power of high frequency components with a threshold level. In this pursuit, a method using dual-window transient energy ratio based on the faulted phase voltage has been presented in [6]. Recently, a criterion based on the differential current of the tripped phase in the transmission line with shunt reactor has been proposed in [7].

In this paper a new method based on discrete wavelet transform (DWT) and correlation coefficient is proposed for distinguishing between arcing and permanent faults.

2. Correlation Coefficient

In practice, the most convenient way to assess the strength dependence between two variables, say, X and Y is through their correlation, defined as:

$$Corr(X,Y)=\frac{Cov(X,Y)}{\sqrt{Var(X)Var(Y)}} \quad (1)$$

For positively correlated variables (e.g., *Corr(X,Y)>0*), there is a tendency for high values of one variable to be associated with high values of the other variable. With negatively correlated variables, there is a tendency for high values of one variable to be associated with low values of the other variables. The strength of these tendencies increases as the correlation moves further away from 0 to 1 or -1 [8].

Received December 29, 2012; Revised February 26, 2013; Accepted March 11, 2013

3. Test System Modelling

The single line diagram of a 400kV transmission line between Anjirak and Abbaspoor substations is shown in Figure 1. The 264km transmission line is modelled by using J. Marti model [9] based on the physical geometry of the line conductors shown in Figure 2.

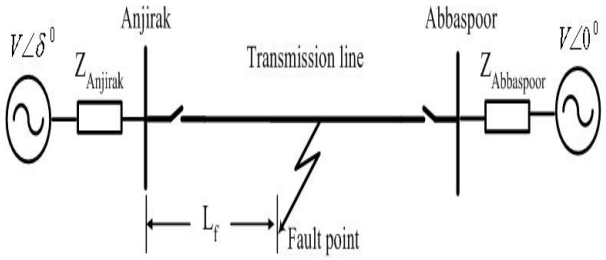

Figure 1. Single Line Diagram of the Simulated Transmission System

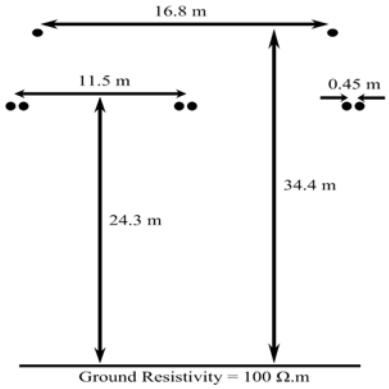

Figure 2. Geometry of the Transmission Line Conductors

The Thevenin equivalent source impedances at the Anjirak and Abbaspoor Buses have been obtained from their short circuit levels. The zero and positive sequence impedances for the source Thevenin equivalent circuits are:

$$Z_{1Anjirak} = 1.7902 + 17.2186\text{i} \ , \ Z_{0Anjirak} = 6.8554 + 20.3674\text{i} \quad (2)$$

$$Z_{1Abbaspoor} = 0.6256 + 8.6006\text{i} \ , \ Z_{0Abbaspoor} = 0.4511 + 5.3909\text{i} \quad (3)$$

Several arcing fault models have been proposed in the literature. Modelling techniques for arc phenomena have improved by field experiments to simulate dynamic characteristics [10, 11].

In this paper, arcing faults have been modelled as presented in [11]. From a modelling point of view, arcing faults can be classified as high current primary arc during the fault and low current secondary arc after the faulted phase is isolated. The secondary arc is sustained by mutual coupling between the healthy and faulted phases [11].

3.1. Primary Arc

It can be shown that the primary arc model is represented by a time dependent resistance as follows:

$$\frac{dg_p}{dt} = \frac{1}{T_p}\left(G_p - g_p\right) \quad (4)$$

Where g_p is the time varying primary arc conductance, T_p is the time constant of the primary arc and G_p is the stationary primary arc conductance.

The stationary primary arc conductance can be defined as:

$$G_p = \frac{|i|}{V_p \ell_p} \quad (5)$$

Where V_p is the constant voltage parameter per unit length of the primary arc, ℓ_p is the primary arc length and $|i|$ is absolute value of the primary arc current.

The time constant of the primary arc can be evaluated by:

$$T_p = \frac{\alpha_P I_p}{l_p} \tag{6}$$

Where the coefficient α_P is about 2.85×10^{-5} for the arc currents ranging from 1.4kA to 24kA [11].

3.2. Secondary Arc

The secondary arc is a highly complex phenomenon, and is influenced by a number of factors [11]. The secondary arc can be modelled by:

$$\frac{dg_s}{dt} = \frac{1}{T_s}\left(G_s - g_s\right) \tag{7}$$

Where g_s is the time varying secondary arc conductance, T_s is the time constant of the secondary arc and G_s is the stationary secondary arc conductance.

The stationary secondary arc conductance is obtained by:

$$G_s = \frac{|i|}{V_s \ell_s(t_r)} \tag{8}$$

Where V_s is the constant voltage parameter per unit length of secondary arc, $\ell_s(t_r)$ is the time varying length of secondary arc and $|i|$ is absolute value of the secondary arc current.

The time constant of the secondary arc can be defined as:

$$T_s = \frac{\beta I_s^{1.4}}{\ell_s(t_r)} \tag{9}$$

Where the coefficient β is about 2.51×10^{-3} for low current arcs [11].

The secondary arc length variation is approximated by the following equation for relatively low wind velocities from 0-1 m/s:

$$\ell_s(t_r)/\ell_{s0} = \begin{cases} 10t_r & t_r > 0.1s \\ 1 & t_r \le 0.1s \end{cases} \tag{10}$$

Furthermore, the re-ignition voltage (withstand voltage) has the complex characteristics of the secondary arc as described in [11]. The secondary arc can be re-ignited if a sustaining arc energy voltage supplied by power system is larger than the re-ignition voltage. Based on the experimental results, the re-ignition voltage is obtained by Equation 11 [11]:

$$V_r(t_r) = \left[5 + \frac{1620\,T_e}{2.15 + I_s}\right] \times (t_r - T_e)\; h(t_r - T_e) \times 10^3\; V/cm \tag{11}$$

Where $V_r(t_r)$ is the arc re-ignition voltage that has to be reached before the arc re-strikes again, T_e is time from the initiation of secondary arc to a current zero and $h(t_r\text{-}T_e)$ is a delayed unit-step function (= 0 when $t_r < T_e$ and = 1 when $t_r > T_e$).

An arcing earth fault on Phase ‘a’ at 35km from Anjirak Substation has been simulated and corresponding voltage of the faulted Phase ‘a’ measured at the Anjirak Bus is illustrated in Figure 3. It can be seen that following the fault occurrence at t_f=0.32s, the bus voltage reduces. At t_b=0.37s, the breaker interrupts the fault current and isolate the faulted phase. The time interval between t_b and t_q illustrates the behaviour of the voltage of the isolated phase during the secondary arc period. At t_q=0.65s the secondary arc is quenched and the recovery voltage Direct Current (DC) offset appears due to the residual voltage of the transmission line. The voltage waveform of the faulted phase is similar to the results obtained in [11], which validates the simulation accuracy of this paper.

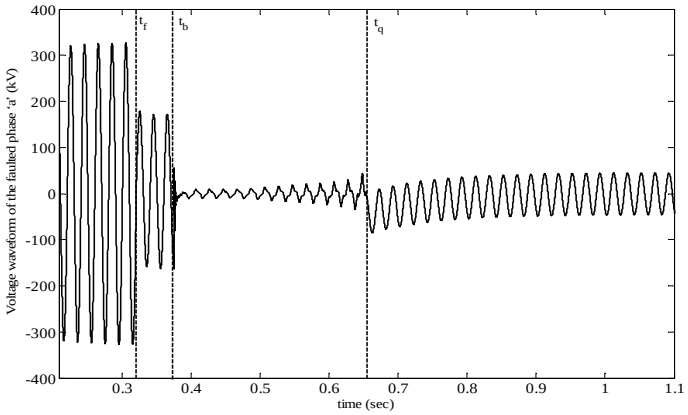

Figure 3. Voltage Waveform of the Faulted Phase ‘a’ for the Single-phase-to-earth Arcing Fault

4. Proposed Method

The proposed method for arcing fault detection is based on DWT and correlation coefficients. The algorithm includes offline and online processing.

4.1. Off line Processing

In the offline, DWT is used to decompose the known faulted phase voltage signal and to generate an index under arcing fault condition. The index is the normalised energy of detail coefficients of faulted phase voltage at resolution levels 1 to 14 as shown below.

To compute the index assume faulted phase voltage signal, S(t), is decomposed to N levels by DWT, as follows:

$$S(t) = S_{c1}(t) + S_{d1}(t) + S_{d2}(t) + S_{d3}(t) + ... + S_{dN}(t) \quad (12)$$

$$S(t) = \sum_i c_1(i)\phi(t-i) + \sum_i \sum_{j=1}^{N} d_j(i) 2^{\frac{j}{2}} \psi\left(2^j t - i\right) \quad (13)$$

In a multi resolution analysis, a set of nested subspaces V_j and W_j are defined as:

$$V_N \supset V_{N-1} \supset V_{N-2} \supset ... \supset V_j \supset ... \supset V_2 \supset V_1 \quad (14)$$

$$V_{j+1} = V_j \oplus W_j \quad (15)$$

$$V_j \cap W_j = \{0\} \quad (16)$$

Where $\oplus$ denotes the summation of two subspaces.

Consequently, an input signal S(t) can be decomposed into its subset signals $S_{c1}(t)$ and $S_{dj}(t)$ in accordance with the subsets V_1 and W_j, respectively, as follows [12]:

$$S_{c1}(t) = \sum_i c_1(i)\phi(t-i) \tag{17}$$

$$S_{dj}(t) = \sum_i d_j(i) 2^{\frac{j}{2}} \psi\left(2^i t - i\right) \tag{18}$$

Where $\phi, \psi \in R$.

Therefore, the energy of detail coefficients of distorted signal S(t) at resolution level j is computed from:

$$E_{dj} = \sum_{i=1}^{N_{dj}} \left| d_j(i) \right|^2 \tag{19}$$

Where *j* is the level of decomposition, d_j and N_{d_j} are the detailed coefficients and number of detailed coefficients at level *j*, respectively. Accordingly, the aforementioned index is defined as:

$$Index = \frac{[E_{d1}, E_{d2}, ..., E_{d13}, E_{d14}]}{Max\left(E_{d1}, E_{d2}, ..., E_{d13}, E_{d14}\right)} \tag{20}$$

Therefore, index is a vector which has fourteen members. This index is computed during the offline processing for the known arcing fault condition. The index will be used in online operation to distinguish between arcing and permanent faults**.** It should be noted that index has been computed after the faulted phase is isolated from both ends by opening the breakers.

4.2. Online Processing

After faulted phase is isolated from the both line ends by opening the breakers, five cycles of the unknown faulted phase voltage is captured using 20 kHz sampling rate. Then the unknown signal is decomposed by db4 to 14 levels to compute the index using Equation 20.

Finally, correlation coefficient between the pre-stored index (calculated in the offline processing) and the computed index of a recorded indistinct signal is calculated. If this correlation coefficient is higher than 0.7, it means that an arcing fault is occurred, otherwise it is a permanent fault.

5. Results and Discussion

Numerous simulation tests under different fault conditions on the test system of Figure 1 have been used to verify the accuracy of the proposed method. The fault conditions include different load angles, line lengths, and fault locations. Only some selected test results are given here for the purpose of brevity.

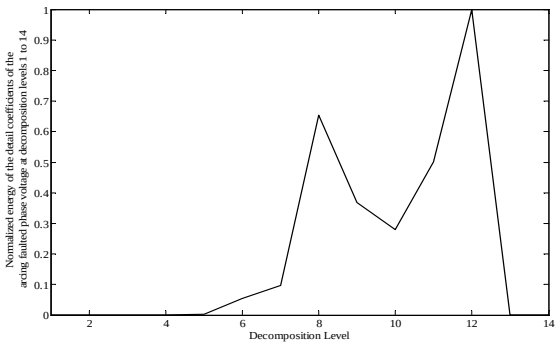

Figure 4. Normalized Energy of the Detail Coefficients of the Arcing Faulted Phase Voltage at Decomposition Levels 1 to 14

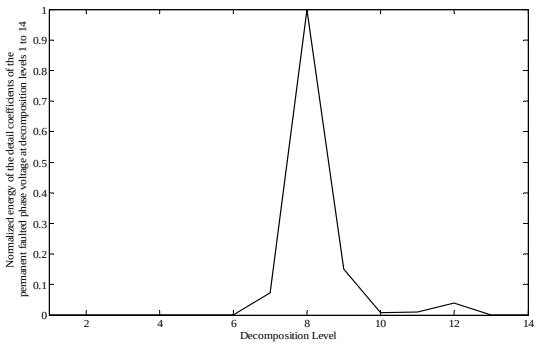

Figure 5. Normalized Energy of the Detail Coefficients of the Permanent Faulted Phase Voltage at Decomposition Levels 1 to 14

Figure 4 shows the index for the arcing fault condition that **a** phase 'a' to earth fault occurs on the transmission line at 0.32s and the faulted phase is isolated at 0.37s from the both ends by opening the breakers. The fault location is at 130km from the line sending end and the load angle is 0^0. Figure 5 shows the index behaviour under permanent fault for the same fault condition. It can be seen in Figure 4 and Figure 5 that the behavior of the index is different under arcing faults and permanent faults. So we can use the correlation coefficient as a tool in distinguishing between arcing faults from permanent faults. The results of application of the proposed algorithm for different arcing fault conditions are shown in Table 1. Table 2 shows correlation coefficients for permanent faults according to the proposed algorithm for different conditions. It can be seen from these Tables that if the correlation coefficient is higher than 0.7, the recorded signal is an arcing fault otherwise it is a permanent fault.

Table 1. Correlation Coefficient Values for Different Arcing Fault Conditions

Load angle (δ^0)	Fault location (L_f), km	Correlation coefficient
0	10	0.9879
0	120	0.9906
0	250	0.9352
-5	10	0.8725
-5	120	0.9023
-5	250	0.8746
5	10	0.9017
5	120	0.9112
5	250	0.8904
-10	10	0.8805
-10	120	0.8978
-10	250	0.8939
10	10	0.9014
10	120	0.9591
10	250	0.8702

Table 2. Correlation Coefficient Values for Different Permanent Fault Conditions

Load angle (δ^0)	Fault location (L_f), km	Correlation coefficient
0	10	0.5039
0	120	0.4868
0	250	0.5644
-5	10	0.5120
-5	120	0.5412
-5	250	0.4291
5	10	0.5763
5	120	0.5281
5	250	0.4995
-10	10	0.4728
-10	120	0.5167
-10	250	0.5594
10	10	0.4812
10	120	0.5379
10	250	0.4906

6. Conclusion

A new and simple method for distinguishing between arcing and permanent faults has been presented. The indistinct signal is sampled, decomposed to 14 levels and its correlation with the pre-stored typical arcing fault is used to recognise the fault type (arcing or permanent fault). Main advantages of the proposed algorithm are:

- Inherent advantages of discrete wavelet transform and correlation coefficient without experiencing limitations associated with conventional neural network (or neural network-fuzzy) based arcing fault detection approaches, such as training, high computing storage and time due to large matrix dimensions.

Fine performance and high accuracy as demonstrated by simulation results for numerous arcing and permanent fault conditions.

Acknowledgement

The study was supported by the Imam Khomeini International University, Qazvin, Iran, under grant no.388041-92.

References

[1] RK Aggarwal, AT Johns, YH Song. *Neural-network based adaptive single-pole autoreclosure technique for EHV transmission systems. IEE Proceedings on Generation Transmission and Distribution.* 1994: 141(2); 243–250.
[2] MB Djuric, VV Terzija. A new approach to the arcing faults detection for fast autoreclosure in transmission systems. *IEEE Trans. Power Del.*, 1995; 10(4): 1793-1798.
[3] ZQ Bo, RK Aggarwal, AT Johns. *A new approach to transient and permanent faults identification based on HF transient*. Proceeding International Conference on Advance in Power System Control, Operation Management. Hong Kong. China. 1995; 189–192.
[4] ZQ Bo, RK Aggarwal, AT Johns. *A new concept in transmission line reclosure using HF fault transient. IEE Proceedings on Generation Transmission and Distribution*. 1997; 144(5): 1–6.
[5] ZQ Bo, RK Aggarwal, AT Johns. *A novel technique to distinguish between transient and permanent fault based on detection of current transients*. Proceeding of 4th International Conference on Advances in Power System Control and Management. Hong Kong. 1997; 217-220.
[6] X Lin, H Liu, H Weng, P Liu, B Wang, ZQ Bo. A Dual-Window Transient Energy Ratio-Based Adaptive Single-Phase Reclosure Criterion for EHV Transmission Line. *IEEE Transactions on Power Delivery.* 2007; 22(4): 2080-2086.
[7] Je Suonan, W Shao, G Song, Z Jiao. A Novel Single-Phase Adaptive Reclosure Scheme for Transmission Lines with Shunt Reactors. *IEEE transactions on power delivery*. 2009; 24(2): 545-551.
[8] AJ Hayter. *Probability and Statistics*, 2nd edition, CA, Wadsworth Group. 2002: 137.
[9] JR Marti. Accurate modeling of frequency-dependent transmission lines in electromagnetic transient simulations. IEEE Transactions on Power Apparatus and Systems. 1982; PAS-101(1): 147–155.
[10] L Prikler, M Kizilcay, G Ban, P Handl. *Improved Secondary Arc Models based on Identification of Arc Parameters from Staged Fault Test Records*. Proc. 14th Power Systems Computation Conf., 2002; 24(3).
[11] AT Johns, RK Aggarwal, Y Song. Improved technique for modelling fault arcs on faulted EHV transmission systems. *IEE Proceedings on Generation Transmission and Distribution*. 1994; 141(2): 148-154.
[12] CS Burrus, RA Gopinath, H Guo. *Introduction to Wavelets and Wavelet Transform: A Primer*. Englewood Cliffs, NJ: Prentice-Hall. 1998.